

---

# UWB-Bandpass Filters with Improved Stopband Performance

---

Mongkol Meeloon, Sarawuth Chaimool and Prayoot Akkaraekthalin

Additional information is available at the end of the chapter

<http://dx.doi.org/10.5772/48736>

---

## 1. Introduction

In wireless communication systems, microwave planar bandpass filters are employed in most applications. The broadband and multiband applications are renewing the interest in the design of planar broadband filters with low loss, compact size, high suppression of spurious responses, and improved stopband performances. However, since the ultra-wideband (UWB) system covers very wide frequency range of 3.1 to 10.6 GHz and then may be interfered with the existing undesired narrow band from the 5.2 GHz or 5.8 GHz wireless local area network (WLAN) radio signals. Moreover, the WiMAX (3.5 GHz) and RFID (6.8 GHz) communications may interfere with the UWB system within the range defined by the FCC. Therefore, UWB bandpass filters with single- and multi-narrow notched bands are needed to avoid being interfered by the exiting RF signals. In order to obtain operations, several techniques have been reported in literatures based on UWB-bandpass filters with slotted resonators (Meeloon et al., 2007, 2008, 2009), UWB-bandpass filters with slotted resonators and embedded slotted feed (Meeloon et al., 2009, 2011), and UWB-bandpass filters with slotted resonators and embedded fold-slot feed (Meeloon et al., 2010, 2011).

In this chapter, many advanced UWB-bandpass filters are presented based on slotted linear tapered-line resonator (SLTR) and slotted step-impedance resonator (SSIR) structures for size reduction and improved stopband performances. A comprehensive treatment of slotted resonators and both ends of the resonator with interdigital coupled lines is described. The design concept is demonstrated using two filter examples including one with an SLTR and another one with an SSIR. These filters have not only compact size but also a wider upper stopband resulting from resonator bandstop characteristics. Single-SLTR and single-SSIR filters are designed and constructed and their performances are extensively investigated in simulation and measurement. The proposed filters demonstrate their capabilities in suppression of spurious responses. Also, two-SLTR and two-SSIR filters are designed and

fabricated to prove that they improve the passband and upper stopband performances with sharpened rejection skirts outside the passband and widened upper stopband.

Then, UWB-bandpass filters based on SLTR and SSIR with embedded slot feed structure for notched band are presented. The embedded slot feed at the end of resonators will be comprehensively described. The proposed filters have narrow notches in the passband, resulting from the embedded slot feed. The center frequencies and bandwidths of the notched band can be easily adjusted by tuning the length and width of the embedded slot parameters. The wider upper stopbands caused by resonator characteristics have been also obtained.

After that, UWB-bandpass filters with single-notched and dual-notched bands and improved stopband performance are proposed using SLTR and SSIR as multi-mode resonator (MMR) and embedded slotted feed. To avoid the existing interferences in the UWB passband, two different embedded slotted feed are employed to obtain two narrow-notched bands. The center frequency and bandwidth of the notched bands can be controlled by adjusting the dimensions of the embedded slotted feed. To further suppress the upper stopband, the defected slot in  $\lambda/2$  stepped impedance resonator fed by interdigital coupled line is introduced. Very good agreements between the measured and simulated filter characteristics have been obtained validating the proposed filter prototypes.

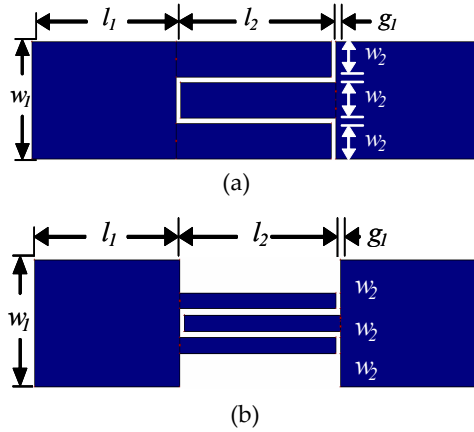
Finally, UWB-bandpass filters based on SLTR and SSIR with embedded fold-slot are presented. The proposed filters have narrow notches in the passband and size reduction, resulting from the embedded fold-slot. The length and width of the embedded fold-slot parameters resulting in their performances have been also studied.

## 2. UWB-bandpass filters with slot resonator

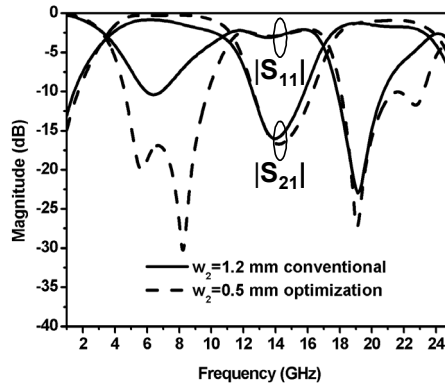
### 2.1. Interdigital coupled line characteristics

Fig. 1(a) shows a conventional interdigital coupled line which has been widely used as a capacitive coupling element in multi-stage bandpass filters. The optimized interdigital coupled lines must be performed to achieve design-specified coupling factor between two adjacent line resonators. The usual procedure is to reduce both strip and slot widths in order to achieve a tight coupling and lower insertion. However, it may introduce some difficulties into the design procedure and fabrication process as the coupling response is sensitive to the strip/slot widths configuration. In this work, we redesign and optimize the interdigital coupled line, as a result shown in Fig. 1(b). An RT/Duroid3003 substrate, which has a given dielectric constant of 3.0, a thickness of 1.524 mm, and a loss tangent of 0.0013 is used for designing the new interdigital coupled lines at a central frequency of 6.85 GHz and a fractional bandwidth of 100%. The conventional and new coupled lines are evaluated by using an electromagnetic simulation program, IE3D, which is based on the method of moments and proven to be quite accurate in its prediction. The response curves of both coupled lines are demonstrated in Fig. 2. It can be noticed that both interdigital coupled lines have almost the same resonant frequency of 6.85 GHz. Nevertheless, the new coupled

line has superior performances with better  $S_{11}$  and  $S_{21}$  in the passband. This means that it is more suited for use as a bandpass filter element than the conventional one.



**Figure 1.** Interdigital coupled lines: (a) conventional one with  $w_1 = 4.0\text{mm}$ ,  $l_1 = 6.0\text{mm}$ ,  $l_2 = 6.45\text{mm}$ ,  $g_1 = 0.2\text{mm}$ , and  $w_2 = 1.2\text{mm}$  and (b) optimized one with  $w_1 = 4.0\text{mm}$ ,  $l_1 = 6.0\text{mm}$ ,  $l_2 = 6.45\text{mm}$ ,  $g_1 = 0.2\text{mm}$ , and  $w_2 = 0.5\text{mm}$ .



**Figure 2.** Compared responses of interdigital coupled lines with  $w_2 = 1.2\text{mm}$  for the conventional one and  $w_2 = 0.5\text{mm}$  for the optimized one.

## 2.2. SLTR and SSIR characteristics

Fig. 3(a) shows a conventional  $\lambda/2$  microstrip linear tapered-line resonator (LTLR). This resonator has inherently spurious resonant frequencies at  $2f_0$  and  $3f_0$ , where  $f_0$  is the fundamental frequency, which may be too close to the desired wide passband. A microstrip SIR has been proposed as shown in Fig. 3(b) for higher stopband performances. In this chapter, microstrip SLTRs as shown in Fig. 3(c) and (d), composed of a microstrip tapered-line with slots are proposed. A microstrip SSIR consisting of a microstrip stepped impedance

line with a slot has been also investigated, as shown in Fig. 3(e). Fig. 4 shows the current densities of resonators at  $3f_0$  about 21 GHz (stopband frequency). We can notice that in Fig. 4(a) and (b), the current densities pass through the resonators. For the proposed resonators in Fig. 4(c) and (d), the current densities cannot pass through the resonators but stop at the slot. It means that the stopband frequency occurs at  $3f_0$ , which is about 21 GHz. We then perform the parameter study for the proposed SLTR and SSIR. The same substrate with the interdigital coupled lines in previous section has been employed. The IE3D program had been used to determine the frequency response of  $S_{21}$ . The input and output ports have been defined at both ends of the proposed resonator. Fig. 5(a) shows the bandstop characteristics of  $S_{21}$  when varying  $w_3$  of the SLTR from 4.5 to 7.5 mm. It can be found that a stopband center can move from the frequency of 24 GHz down to 15.5 GHz. As we can see that the slot is longer, lower stopband center can be obtained due to the slot length affects the distance of current distribution in resonator. When varying  $g_2$  of the SLTR, a stopband center is slightly shifted as shown in Fig. 5(b). Fig. 6(a) and (b) shows bandstop characteristics of the SSIR when varying  $w_3$  and  $g_2$ . The results are same with responses of the SLTR but better  $S_{21}$  magnitudes.

In order to obtain good stopband characteristics without passband perturbations of the desired UWB-bandpass filters, slot length  $w_3 = 5.5\text{mm}$  and slot width  $g_2 = 0.2\text{mm}$  have been chosen as optimized parameters. It can be clearly noticed that the conventional microstrip resonators and the SIR have not obtained stopband characteristics while the proposed slotted resonators have stopband responses with various resonant frequencies. With these stopband characteristics, superior suppression of the spurious responses in the upper band could be obtained when they have been applied to the proposed bandpass filters.

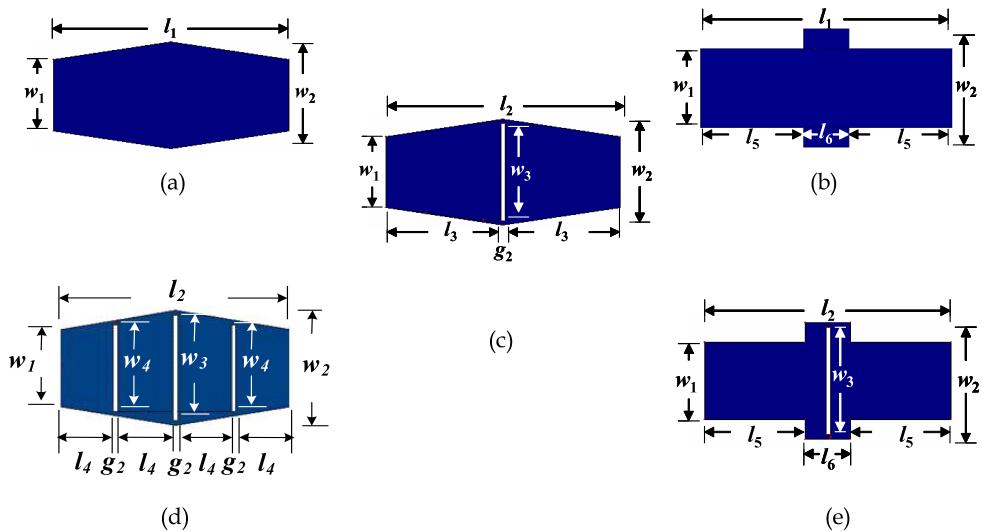


**Figure 3.** (a) a conventional linear tapered-line resonator, (b) a conventional SIR, (c) the proposed SLTR, (d) the proposed SLTR with three slots, and (e) the proposed SSIR. The dimensions are as follows:  $l_1 = 14.0\text{mm}$ ,  $l_2 = 11.0\text{mm}$ ,  $l_3 = 5.4\text{mm}$ ,  $l_4 = 3.47\text{mm}$ ,  $l_5 = 4.5\text{mm}$ ,  $l_6 = 2\text{mm}$ ,  $w_1 = 4\text{mm}$ ,  $w_2 = 6\text{mm}$ ,  $w_3 = 5.5\text{mm}$ ,  $w_4 = 4.5\text{mm}$ , and  $g_2 = 0.2\text{mm}$

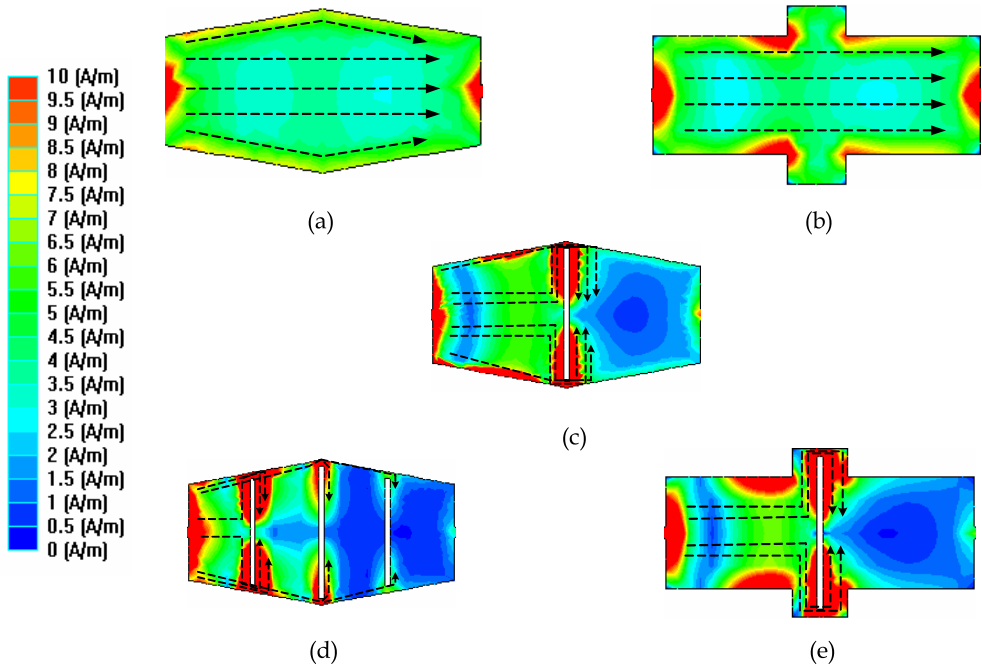


**Figure 4.** Current densities of resonators: (a) a conventional linear tapered-line resonator, (b) a conventional SIR, (c) the proposed SLTR, (d) the proposed SLTR with three slots and (e) the proposed SSIR

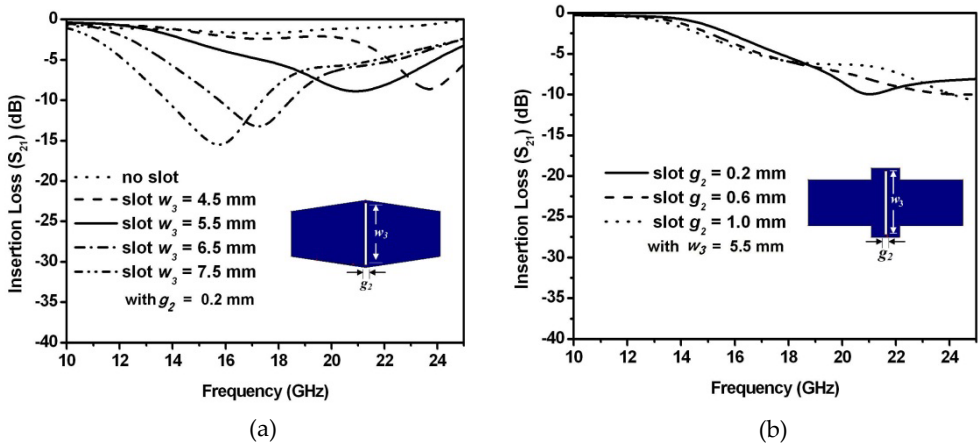


**Figure 5.** Bandstop characteristics at  $3f_0$ : (a) SLTR with varied  $w_3$  and (b) SLTR with varied  $g_2$

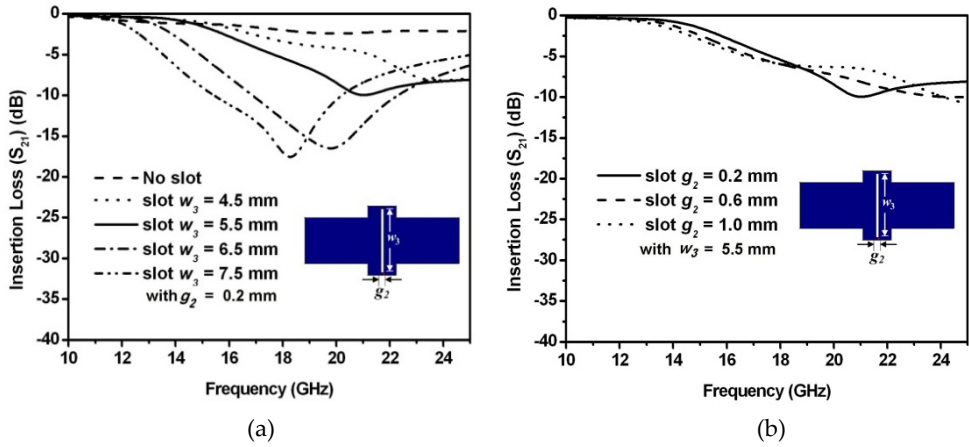


Figure 6.  $S_{21}$  responses: (a) SSIR with varied  $w_3$  and (b) SSIR with varied  $g_2$

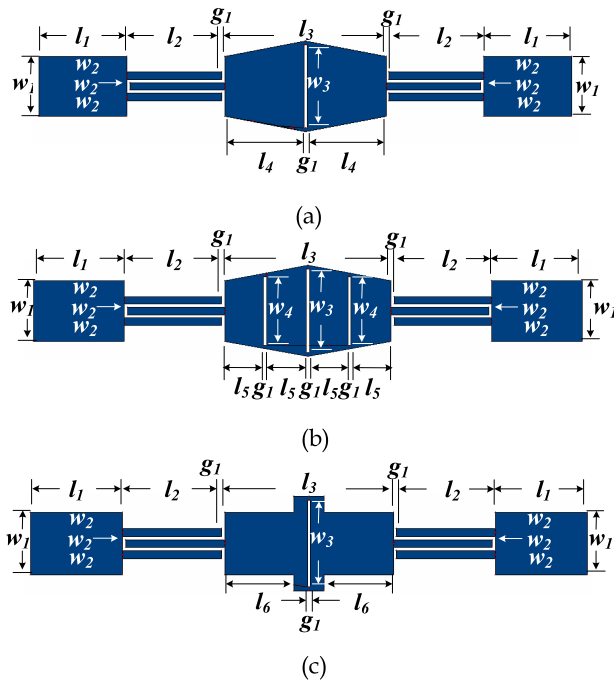


Figure 7. Bandpass filters with a single resonator using: (a) the SLTR (b) the SLTR with three slots, and (c) the SSIR. The dimensions as follows:  $l_1=6.0\text{mm}$ ,  $l_2=6.45\text{mm}$ ,  $l_3=11.0\text{mm}$ ,  $l_4=5.4\text{mm}$ ,  $l_5=3.47\text{mm}$ ,  $l_6 = 4.5\text{mm}$ ,  $w_1 = 4.0\text{mm}$ ,  $w_2 = 0.2\text{mm}$ ,  $w_3 = 5.5\text{mm}$ ,  $w_4 = 4.5\text{mm}$ , and  $g_1 = 0.2\text{mm}$

### 2.3. Filter designs and measured results

#### 2.3.1. Single-SLTR filter

In the following, the two UWB-bandpass filters have been built using the MMR conventional  $\lambda/2$  resonators and the proposed SLTR and SLTR with three slots fed by  $\lambda/4$  interdigital coupled lines at both ends with a central frequency of 6.85 GHz and a fractional bandwidth of 100% as shown in Fig. 7(a) and (b). The RT/Duroid 3003 substrate with a dielectric constant of 3.0, a thickness of 1.524mm and a loss tangent of 0.0013 has been used. The optimized dimensions of the resonators and the interdigital coupled lines have been obtained in the previous section. Their electrical performances are then simulated by using IE3D program.

#### 2.3.2. Single-SSIR filter

Fig. 7(c) shows schematics of the the proposed single-microstrip SSIR bandpass filters. The optimized dimensions of the resonators and the interdigital coupled lines are the same as resulting from the previous section.

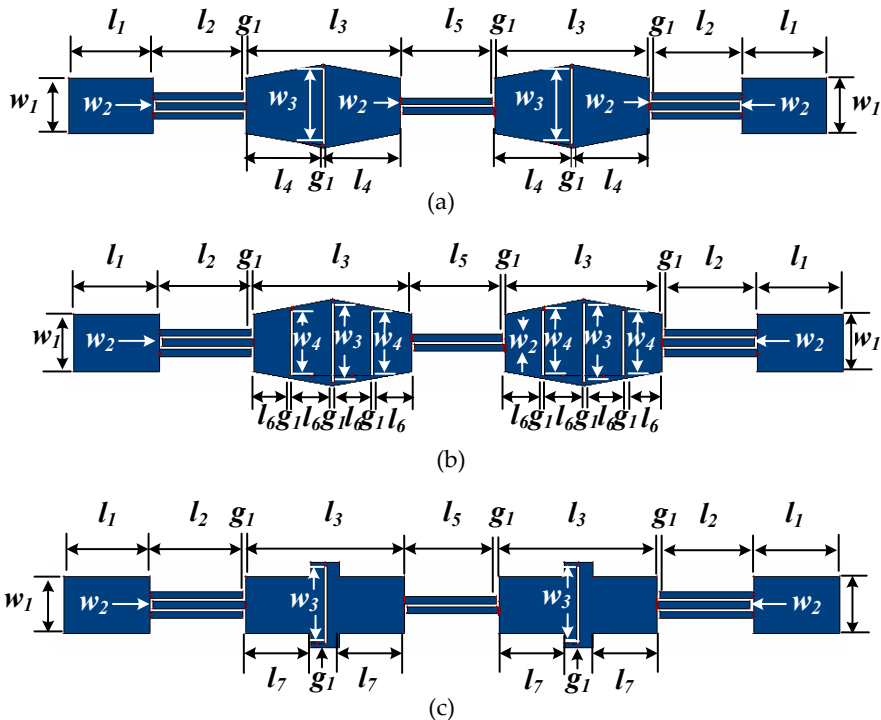


**Figure 8.** Two-resonator bandpass filters: (a) the SLTR with one slot, (b) the SLTR with three slots, and (c) the SSIR. The dimensions are as follows:  $l_1=6.0\text{mm}$ ,  $l_2=6.45\text{mm}$ ,  $l_3=11.0\text{mm}$ ,  $l_4=5.4\text{mm}$ ,  $l_5=6.5\text{mm}$ ,  $l_6=3.47\text{mm}$ ,  $l_7=4.5\text{mm}$ ,  $w_1 = 4.0\text{mm}$ ,  $w_2 = 0.2\text{mm}$ ,  $w_3 = 5.5\text{mm}$ ,  $w_4 = 4.5\text{mm}$ , and  $g_1 = 0.2\text{mm}$

### 2.3.3. Two-SLTR filter

Fig. 8 depicts schematics of the bandpass filters with two linear tapered-line resonators connected in cascade. Fig. 8 (a) and (b) was the proposed SLTR filters with single- and three-slotted structures, respectively. All dimensions of the resonators and interdigital coupled lines have been shown.

### 2.3.4. Two-SSIR filter

Fig. 8(c) depicts schematics of the proposed two-SSIR bandpass filter. The dimensions of the resonators and the interdigital coupled lines are the same.

## 2.4. Experimental verification

In this section, six UWB-bandpass filters are implemented on the RT/Duroid 3003 with a substrate thickness of 1.524 mm, and a dielectric constant of 3.0 at a central frequency of 6.85 GHz and a fractional bandwidth of 100%. Fig. 9 and Fig. 10 shows photographs of the fabricated SLTR and SSIR filters. Fig. 11 shows comparisons of measured and simulated responses of the SLTR and SSIR filters. In Fig. 11(a), (b) and (c), it can be found that the measured results agree very well with the simulation expectations, confirming that the proposed UWB-SLTR and SSIR bandpass filter is capable of reducing the insertion losses within the passband and also widening the upper stopband. The measured return and insertion losses are found to be higher than 14 dB and less than 2 dB over the UWB-passband, respectively. In Fig. 11(d), (e) and (f), two-SLTR and SSIR filter shows the improved upper stopband performance, with the return losses higher than 15 dB inside the passband. The lower and upper band skirts get sharpened to a great extent, while the upper stopband with the insertion losses above 15 dB occupies an enlarged range of 11.3–25 GHz. Also, the proposed two-SLTR filter with three slots has an improved upper stopband performance, as shown in Fig. 11 (e). A two- SSIR filter has improved the upper stopband performances, with the return losses higher than 15 dB outside the UWB-passband, and

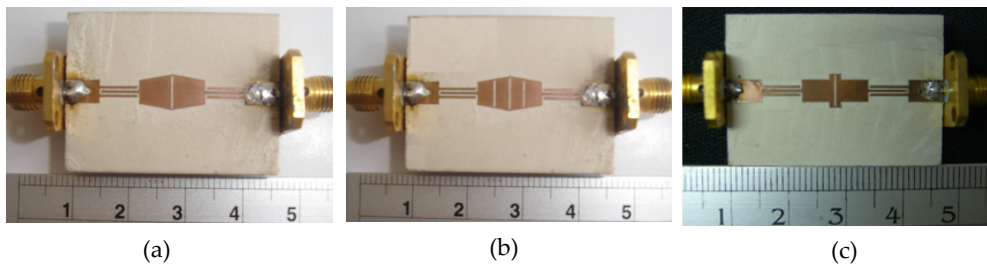
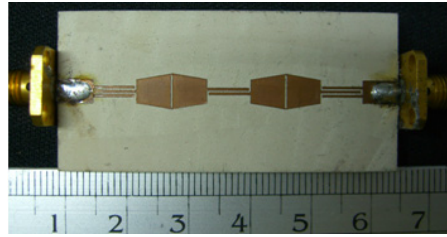
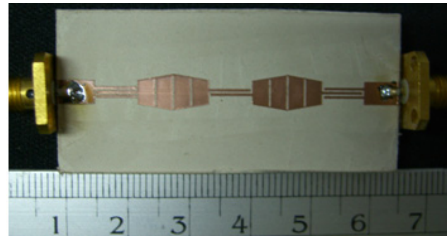


**Figure 9.** Photographs of the fabricated single-filters: (a) single-SLTR, (b) single-SLTR with three slots, and (c) single-SSIR

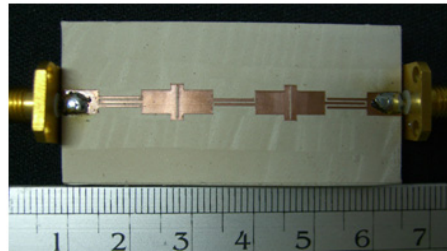




(a)



(b)



(c)

**Figure 10.** Photographs of the fabricated two-filters: (a) two-SLTR, (b) two-SLTR with three slots, and (c) two-SSIR

insertion losses above 25 dB in a range of 19–25 GHz and above 47 dB at 24 GHz as shown in Fig. 11 (f). However, the measured passband insertion loss is higher than the simulation result due to the dimension of the conductor and further the conductivity slightly deviated from the design. The group delay of both filters slightly varies between 0.2 and 0.3 ns in the passband.

### 3. UWB-bandpass filters with embedded slot

This section proposes new UWB-bandpass filters using slotted linear tapered-line resonators (SLTR) and slotted step-impedance resonator (SSIR) structures driven by interdigital coupled lines at both ends of the resonators for improving the stopband performances. Also, using embedded slot structure in the input and output feed line can create a notched band.

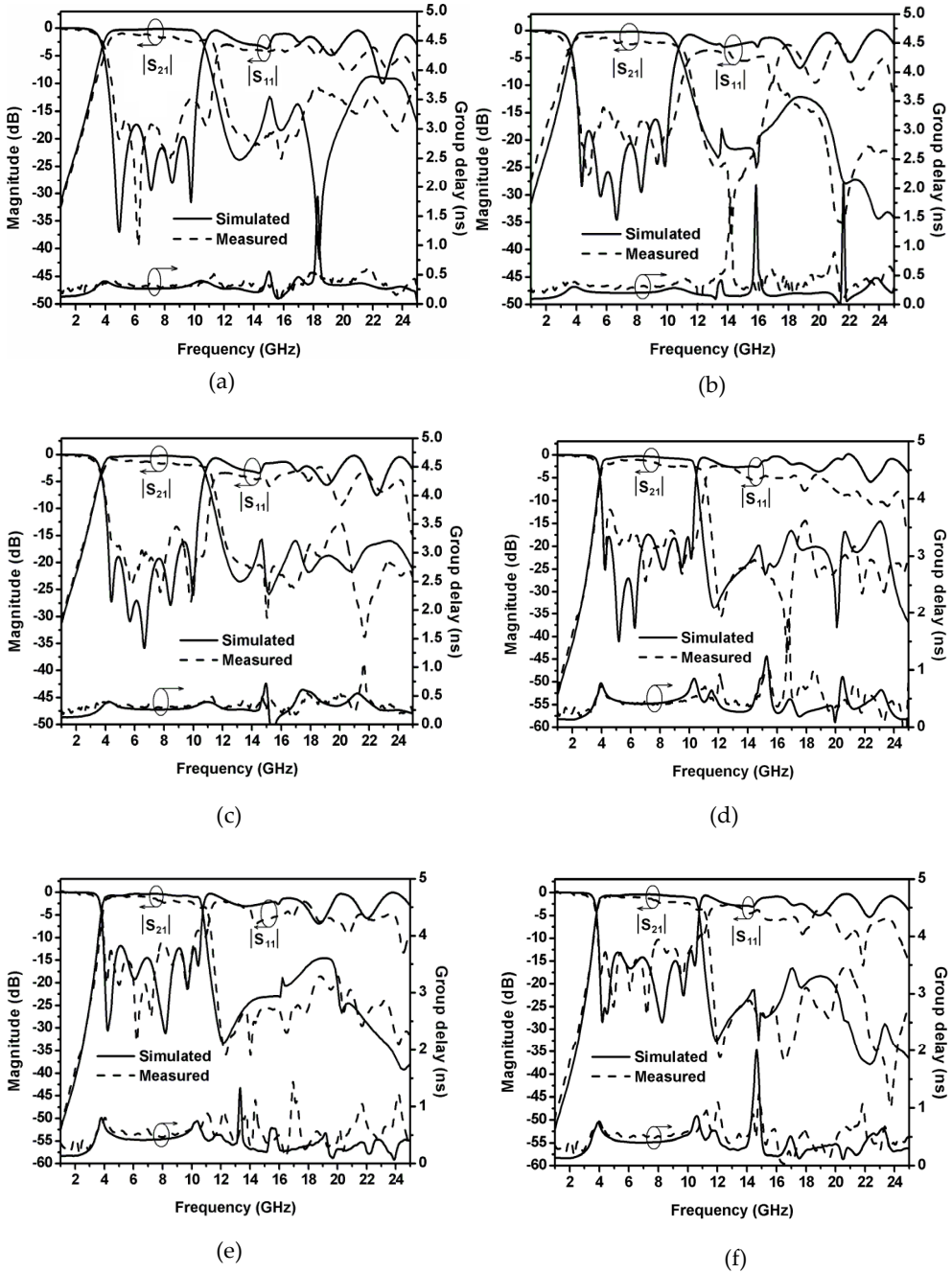


**Figure 11.** Comparisons of measured and simulated responses of the filters: (a) single-SLTR, (b) single-SLTR with three slots, (c) single-SSIR, (d) two-SLTR, (e) two-SLTR with three slots and (f) two-SSIR

### 3.1. Embedded slot feed characteristics

The embedded slot at the feed line has been proposed in order to form a notch band. The RT/Duroid 3003 substrate has been used in this study. Fig.12 (a) shows the part of embedded slot feed and its frequency responses of  $S_{21}$  when varying the length  $L$  of the embedded slot from 5 to 10 mm. It can be found that a center frequency of notched frequency can be adjusted from 9 GHz down to 5 GHz. When increasing the width  $W$  of the embedded slot while keeping the center frequency to be the same, the bandwidth of notched band is increased as shown in Fig. 12 (b). The summary of geometry parameters for the embedded slot structure when varying the width  $W$  of the embedded slot from 0.6 to 1.6 mm and varying the length  $L$  of the embedded slot from 8.593 to 8.393 mm is shown in Table.1. It can be clearly seen that at 3 dB bandwidth of the notched band is increased from 220 to 810 MHz. Therefore, by tuning the length and width of the embedded slot, center frequencies and bandwidth of notched band can be easily adjusted. Embedded slot is thus suitable for use in the UWB-bandpass filter when a notched band is required. To create the notched band at 5.6 GHz, the dimensions of the proposed embedded slot feed include  $l = 8.543$  mm,  $w = 0.8$  mm, and  $g = 0.2$  mm.

To verify the notched mechanism, the current distributions of embedded structure at 5.6 GHz notch frequency are shown in Fig.13. We can notice that in Fig. 13 (a) the current distribution passes through the conventional feed line but it cannot pass through the proposed structure as shown in Fig.13 (b).

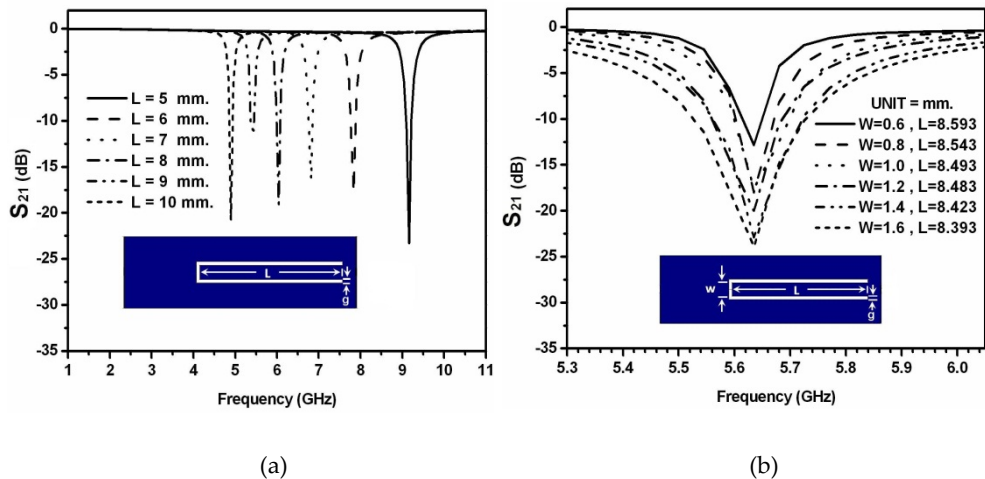


**Figure 12.**  $S_{21}$  magnitude responses of the embedded slot structure with a slot of 0.2 mm when: (a) varying  $L$  (b) varying  $W$

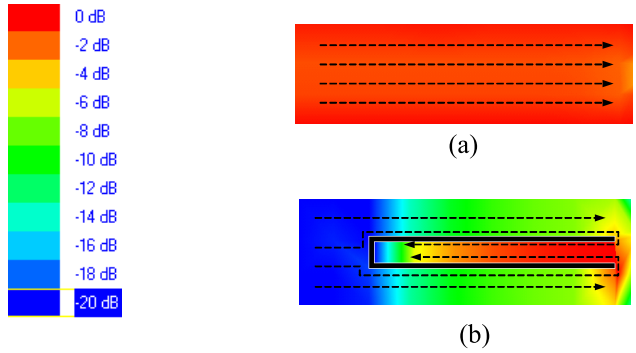


**Figure 13.** Current distribution at 5.6 GHz of embedded structure: (a) a conventional feed line and (b) the proposed embedded structure

W(mm)	L(mm)	BW(MHz)<-3 dB
0.6	8.593	220
0.8	8.543	250
1.0	8.493	360
1.2	8.483	470
1.4	8.423	720
1.6	8.393	810

**Table 1.** Geometry parameters for the embedded slot structure

### 3.2. Filter designs and measured results

#### 3.2.1. SLTR filter with three slots and embedded slot

The UWB-bandpass filters using slotted linear tapered-line resonators (SLTR) with three slots are proposed. The filters consists of the interdigital coupled lines at both ends of the resonators for improving the stopband performances. Also, using embedded slot structure in the input feed line can create a notched band. Fig.14 (a) shows the SLTR with three slots and one embedded slot at the input feed for notched band. The two-cascaded SLTR with three slots and one embedded slot at input feed is also shown in Fig. 14 (b). All dimensions of the UWB-bandpass filters have been shown.

#### 3.2.2. SSIR filter with embedded slot

Fig.14 (c) shows the SSIR with one embedded slot at the input feed for notched band. The SSIR with embedded slot at input and output feed for dual-notched is also shown in Fig.14(d). This section proposes UWB-bandpass filters using slotted step-impedance resonator (SSIR) driven by interdigital coupled lines at both ends of the resonators for improving the stopband performances. Also, using embedded slot structure in the feed line can create a notched band.

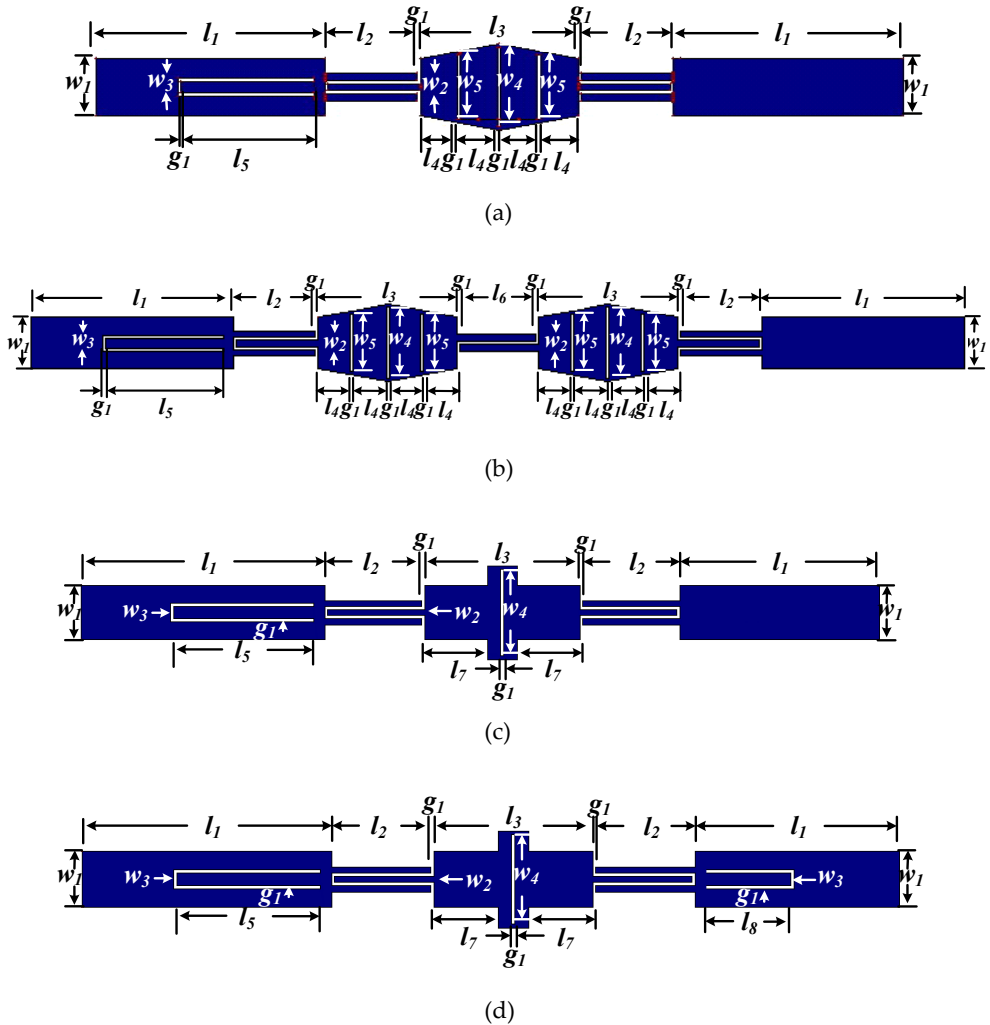
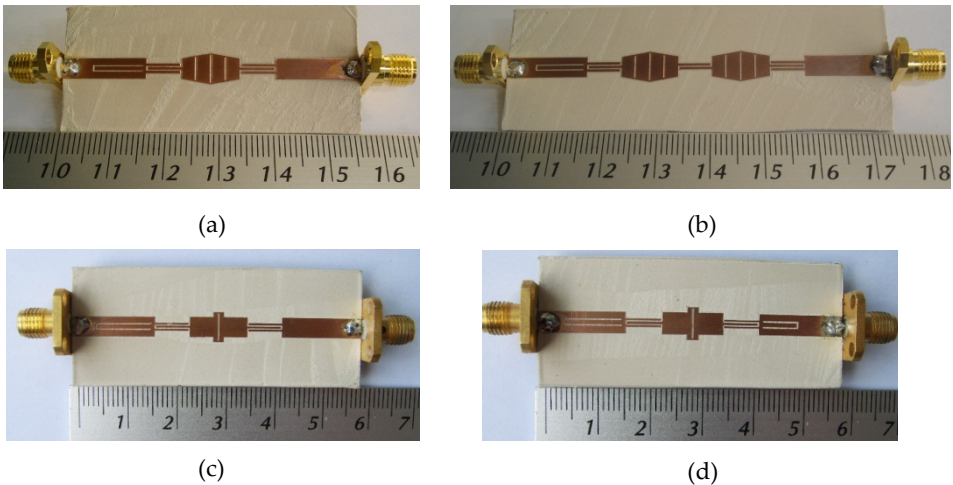


**Figure 14.** The proposed filters for notched band: (a) single-SLTR, (b) two-SLTR, (c) single-SSIR and (d) single-SSIR with dual-notched band. The dimensions are as follows:  $l_1=16.0\text{mm}$ ,  $l_2=6.45\text{mm}$ ,  $l_3=11.0\text{mm}$ ,  $l_4=3.47\text{mm}$ ,  $l_5=8.543\text{mm}$ ,  $l_6=6.5\text{mm}$ ,  $l_7=4.5\text{mm}$ ,  $l_8=5.54\text{mm}$ ,  $w_1=4.0\text{mm}$ ,  $w_2=0.5\text{mm}$ ,  $w_3=0.8\text{mm}$ ,  $w_4=5.5\text{mm}$ ,  $w_5=4.5\text{mm}$  and  $g_1=0.2\text{mm}$

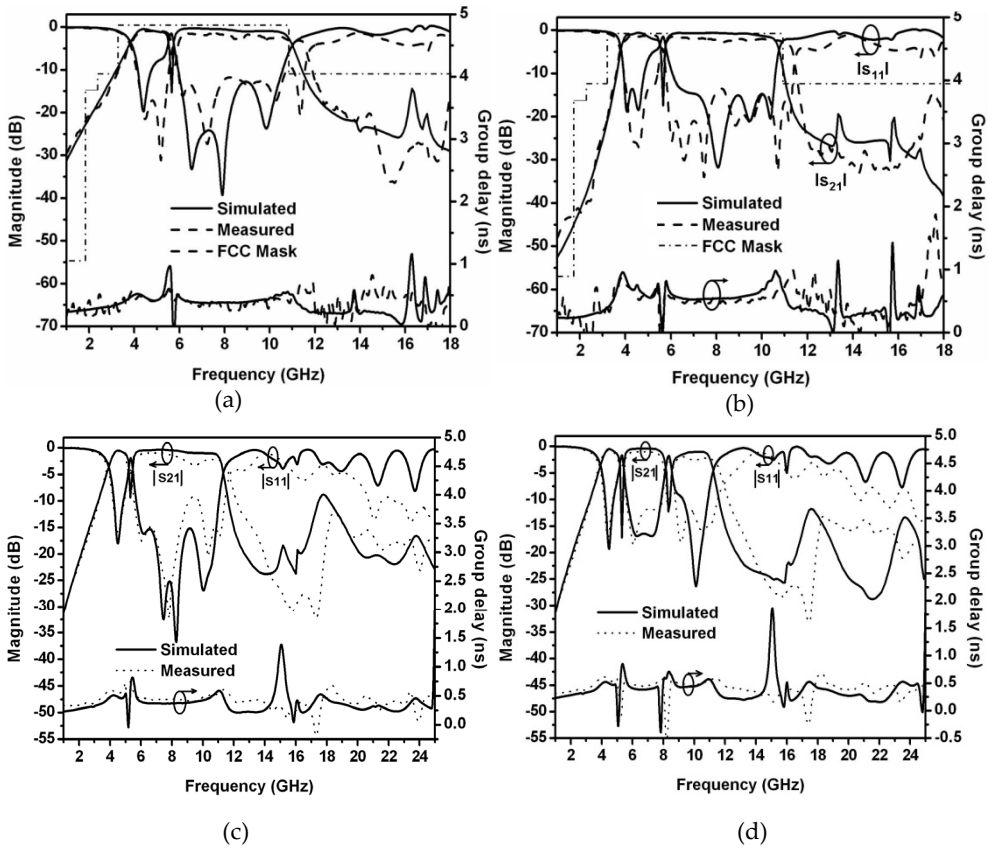
### 3.3. Experimental verification

Fig.15 (a) shows photograph of the fabricated single-SLTR for notched band. Fig. 16 (a) shows a comparison of measured and simulated responses of the single-SLTR filter with a notched band. The measured results are agreed very well with the simulation predictions,

confirming that the proposed SLTR filter with a notch is capable of narrow notched band, good insertion losses within the passband and also widening the upper stopband. The measured return and insertion losses are found to be lower than 10 dB and higher than 2 dB over desired UWB passband, respectively. Fig. 15 (b) shows photograph of the fabricated two-SLTR filter. Fig. 16 (c) shows a comparison of measured and simulated responses of the two-SLTR filter, which a good agreement has been obtained for passband and sharp rejection skirt in upper stop band. The measured return and insertion losses of the two-SLTR filter are found to be higher than 2 dB and lower than 10 dB at the notched frequencies about 5.6 GHz which the bandwidth of notched band are about 276 MHz. Fig. 15 (c) and (d) show photograph of the fabricated SSIR filter with single and dual-notched band. Fig. 16 (c) and (d) show a comparison of measured and simulated responses of the SSIR filters with single and dual-notched band at the notched frequencies about 5.6 GHz and 8.3 GHz which the bandwidth of notched band are about 276 MHz and 300 MHz, respectively. The proposed filters show improved upper stopband performance with high insertion loss. The upper stopband with the insertion loss lower than 15 dB occupies an enlarged range of 12 to 18 GHz. As we can see that the proposed filter exhibits notched and dual-notched band, a wide upper stopband with values of  $S_{21}$  lower than 30 dB at 15 GHz, 10 dB at about 18 GHz. These superior upper stopband performances are caused by the stopband characteristics of the proposed slotted resonator structure and narrow notched band by embedded slot structure. The group delay of fourth filters slightly varies between 0.2 and 0.3 ns in the passband.



**Figure 15.** Photographs of fabricated UWB filters for notched band: (a) single-SLTR, (b) two-SLTR, (c) single-SSIR and (d) single-SSIR with dual-notched band



**Figure 16.** Comparisons of measured and simulated responses of the filters: (a) single-SLTR, (b) two-SLTR, (c) single-SSIR and (d) single-SSIR with dual-notched band

## 4. UWB-bandpass filters with embedded fold-slot

By modifying the UWB-bandpass filters with embedded slot, the embedded slot can be reduce size using embedded fold-slot. It usies slotted linear tapered-line resonator (SLTR) and slotted step-impedance resonator (SSIR) driven by interdigital coupled lines at both ends of the resonator to improve the stopband performances.

### 4.1. Embedded fold-slot feed characteristics

The embedded fold-slot at the input feed has been proposed in order to form a notch band. The RT/Duroid 3003 substrate has been used in this study. Therefore, by tuning the length and width of the embedded slot from previous section, center frequencies and bandwidth of notched band can be easily adjusted. Embedded fold-slot is thus suitable for use in the

UWB- bandpass filter when a notched band is required. To create the notched band at 5.6 GHz, the dimensions of the proposed embedded fold-slot feed include  $l_{11} = 5.94$  mm,  $w_5 = 0.8$  mm, and  $g_1 = 0.2$  mm. To verify the notched mechanism, the current distributions of embedded fold-slot structure at 5.6 GHz notch frequency are shown in Fig. 17. We can notice that in Fig. 17 (a) and (b) the current distribution cannot pass through the embedded slot feed line and the embedded fold-slot feed line.

## 4.2. Filter designs and measured results

### 4.2.1. SLTR filter with embedded fold-slot

The UWB-bandpass filters using slotted linear tapered-line resonators (SLTR) driven by interdigital coupled lines at both ends of the resonators for improving the stopband performances and using embedded fold-slot structure in the input feed line can create a notched band are proposed. Fig.18 (a) and 18 (b) show the SLTR and SLTR filters with three slots, using embedded fold-slot at the input feed for notched band. The two-cascaded SLTR with embedded fold-slot at input feed is also shown in Fig. 18 (c). All dimensions of the UWB-bandpass filters have been shown.

### 4.2.2. SSIR filter with embedded fold-slot

Fig. 18 (d) shows the SSIR with embedded fold-slot at the input feed for notched band.

This section proposes a new UWB-bandpass filter with simple structures using slotted step-impedance resonator (SSIR) driven by interdigital coupled lines at both ends of the resonators for improving the stopband performances. Also, using embedded fold-slot in the input feed line can create a notched band.

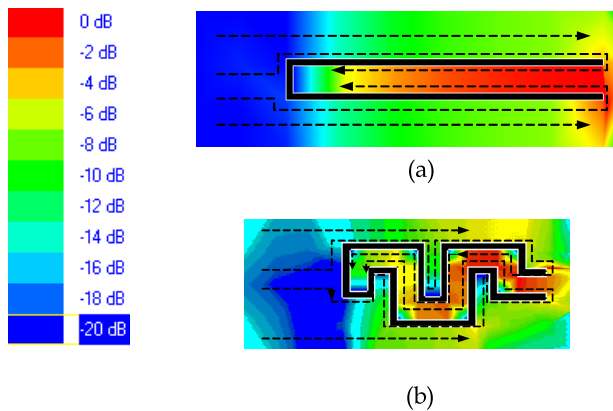


**Figure 17.** Current distribution at 5.6 GHz of embedded structure: (a) the embedded structure, (b) the proposed embedded fold-slot structure



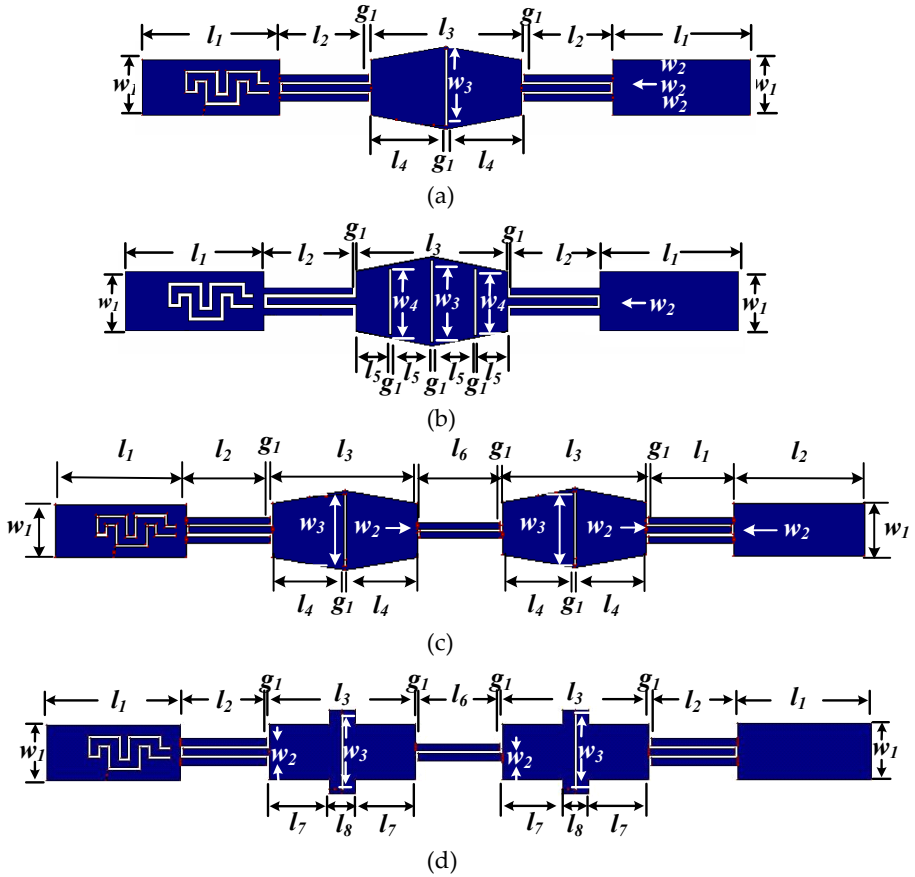


**Figure 18.** The proposed filters for notched band: (a) single-SLTR, (b) single-SLTR with three slot (c) two-SLTR, and (d) two-SSIR. The dimensions are as follows:  $l_1=10.0\text{mm}$ ,  $l_2=6.45\text{mm}$ ,  $l_3=11.0\text{mm}$ ,  $l_4=5.4\text{mm}$ ,  $l_5=3.47\text{mm}$ ,  $l_6=6.5\text{mm}$ ,  $l_7=4.5\text{mm}$ ,  $l_8=2.0\text{mm}$ ,  $l_9=2.12\text{mm}$ ,  $l_{10}=1.47\text{mm}$ ,  $l_{11}=5.94\text{mm}$ ,  $w_1=4.0\text{mm}$ ,  $w_2=0.5\text{mm}$ ,  $w_3=5.5\text{mm}$ ,  $w_4=4.5\text{mm}$ ,  $w_5=0.5\text{mm}$ ,  $w_6=2.1\text{mm}$ ,  $w_7=0.52\text{mm}$  and  $g_1=0.2\text{mm}$

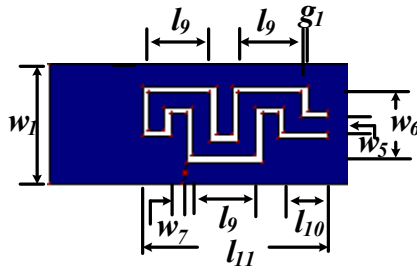


**Figure 19.** Embedded fold-slot feed

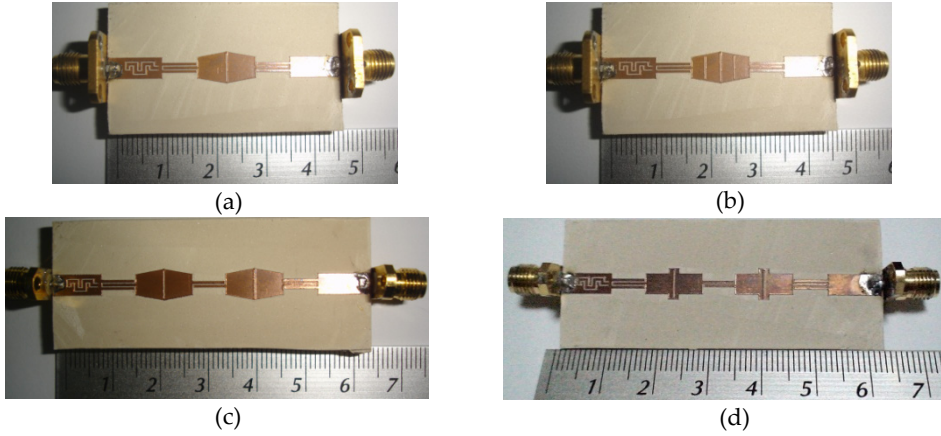


**Figure 20.** Photographs of fabricated UWB-filters for notched band: (a) single-SLTR, (b) two-SLTR, (c) two-SLTR and (d) two-SSIR

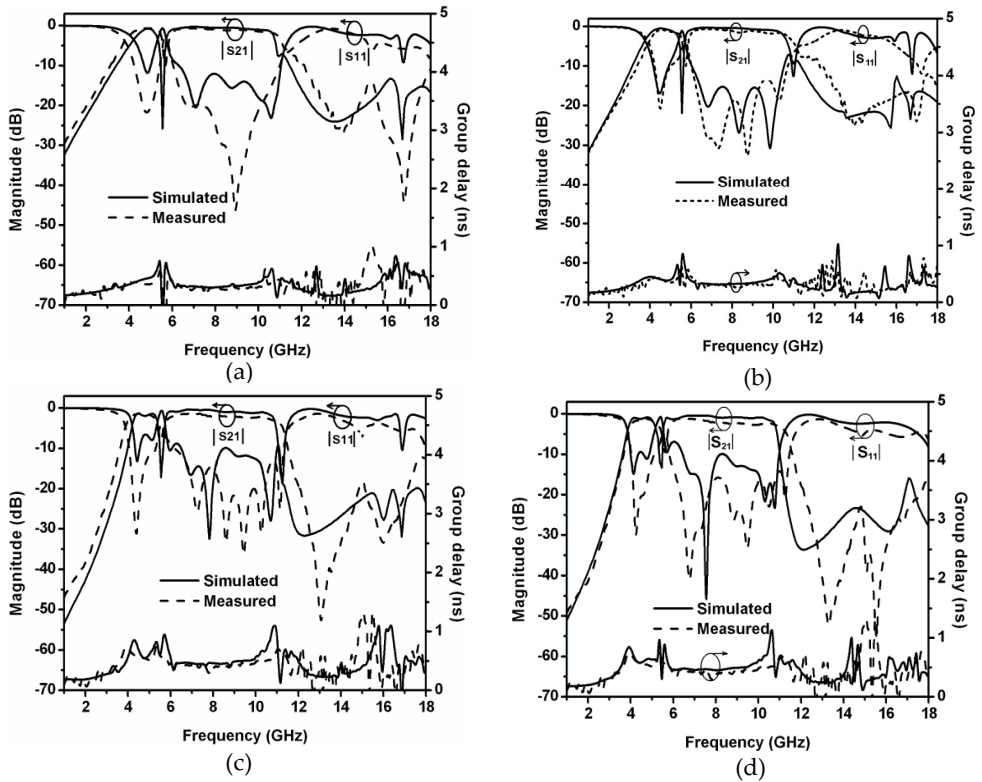


**Figure 21.** Comparisons of measured and simulated responses of the filters: (a) single-SLTR, (b) single-SLTR with three slots, (c) two-SLTR, (d) two-SSIR

### 4.3. Experimental verification

Fig. 20 shows the photograph of the fabricated SLTR and SSIR filters for notched band. Fig. 21 shows a comparison of measured and simulated responses of the SLTR and SSIR filters with a notched band. The measured and simulated results have shown good agreement with a notch is capable of narrowing notched band, having good insertion losses within the passband and also widening the upper stopband. The measured return and insertion losses are found to be lower than 10 dB and higher than 2 dB, respectively over desired UWB-passband. The notched frequency of about 5.6 GHz has a bandwidth of about 276 MHz. The proposed filters show narrow notched band and improved upper stopband performance with high insertion loss. The upper stopband with the insertion loss lower than 10 dB occupies an enlarged range of 14 to 18 GHz. The group delay of both filters slightly varies between 0.2 to 0.3 ns in the passband. These superior stopband performances are caused by the stopband characteristics of the proposed slotted resonator structure, and narrow notched band is caused by embedded fold-slot structure.

## 5. Conclusion

In this chapter, the novel SLTR and SSIR UWB-bandpass filters with improved upper stopband performances have been presented and implemented. By properly forming SLTR and SSIR together with two interdigital coupled lines at both ends, the proposed filters are designed and constructed. The single-SLTR and SSIR filters show their performances in suppression of spurious responses. Also, two-SLTR and two-SSIR filters are designed and fabricated to show that they improve the passband and upper stopband performances with sharpened rejection skirts outside the passband and widened upper stopband. When comparing with SLTRs, we find that the SSIR structures are easier to design and fabricate and they also have better stopband characteristics. In addition, the SLTR and SSIR filters using embedded slot and embedded fold-slot with notched band, reduce size and improved upper stopband performances have been presented and implemented. The proposed filters demonstrate their capability in narrow notched band with the embedded slot, embedded fold-slot feed and suppression of spurious responses with slotted resonators. Also, the fabricated filters prove that they can create notched band and improve upper stopband performances with sharpened rejection and widen the upper stopbands.

### Author details

Mongkol Meeloon

*Department of Special Investigation (DSI), Thailand*

Sarawuth Chaimool and Prayoot Akkaraekthalin

*King Mongkut's University of Technology, North Bangkok, Thailand*

## 6. References

- Meeloon, M.; Akkaraekthalin, P. (2007). Broadband bandpass filters using slotted linear tapered-line resonators for improving upper stopband performances, *Proceedings of EECON-30 30<sup>th</sup> Electrical Engineering conference*, pp.1109-1112, Kanchanaburi, Thailand, 2007
- Meeloon, M.; Chaimool, S.; Akkaraekthalin, P. (2007). Broadband bandpass filters using slotted resonators fed by interdigital couple line for improving upper stopband performances, *Proceedings of APMC 2007 Asia-Pacific Microwave conference*, Bangkok, Thailand, 2007
- Meeloon, M.; Chaimool, S.; Akkaraekthalin, P. (2008). Broadband bandpass filters using slotted stepped impedance resonators for improving upper stopband performances, *Proceedings of ECTI-CON2008 5<sup>th</sup> International Conference on Electrical Engineering/Electronics, Computer, Telecommunications and Information Technology*, pp.265-268, Krabi, Thailand, 2008
- Meeloon, M.; Chaimool, S.; Akkaraekthalin, P. (2009). Broadband bandpass filters using slotted resonators fed by interdigital coupled lines for improved upper stopband performances, *AEU International Journal of Electronics and Communications*, vol. 63, pp.454-463, 2009
- Meeloon, M.; Chaimool, S.; Akkaraekthalin, P. (2009). A Broadband bandpass filter with a notch-band using step-impedance resonator and embedded slots, *Proceedings of APMC 2009 Asia-Pacific Microwave conference*, pp.1446-1449, Singapore, 2009
- Meeloon, M.; Chaimool, S.; Akkaraekthalin, P. (2009). Broadband bandpass filters with notched bands using embedded slots, *Proceedings of EECON-32 32<sup>th</sup> Electrical Engineering conference*, Nakhon Nayok, Thailand, 2009
- Meeloon, M.; Chaimool, S.; Akkaraekthalin, P. (2011). Ultra-wideband bandpass filters with notched using slotted linear tapered-line resonators and embedded slot feed, *Proceedings of ECTI-CON2011 8<sup>th</sup> International Conference on Electrical Engineering/Electronics, Computer, Telecommunications and Information Technology*, pp.244-247, Khon Kaen, Thailand, 2011
- Meeloon, M.; Chaimool, S.; Akkaraekthalin, P. (2010). Broadband bandpass filters with notched bands using embedded fold-slot, *Proceedings of EECON-33 33<sup>th</sup> Electrical Engineering conference*, Chiang Mai, Thailand, 2010
- Meeloon, M.; Chaimool, S.; Akkaraekthalin, P.; Leenaphet, A.; Pattanakun, R. (2011). An Ultra-wideband bandpass filter with notched using step-impedance resonators and embedded fold-slot, *Proceedings of ISAP-2011 International Symposium on Antennas and Propagation*, Jeju, Korea, 2011
- Meeloon, M.; Jeeracheeweeikul, V.; Mahatthanathawee, S.; Ngamkhum, J.; Chomputawat, A.; Chomputawat, S.; Rattarasarn, M. (2011). An Ultra-wideband bandpass filter with notched band using embedded fold-slot feed and three-slotted resonator, *Proceedings of ISPACS-2011 International Symposium on Intelligent Signal Processing and Communication Systems*, Chiang Mai, Thailand, 2011